doi: 10.5937/SimTerm24324N

Heat Transfer Effects on the EMHD Flow of Ternary Hibrid Nanoluid in the Channel with Porous Medium

Milica Nikodijević Đorđević[a], Jelena Petrović[b], Miloš Kocic[c], Živojin Stamenković[d]

[a]*Faculty of Occupational Safety, Niš, RS, milica.nikodijevic@znrfak.ni.ac.rs,*
[b]*Faculty of Mechanical Engineering, Niš, RS, jelena.nikodijevic.petrovic@masfak.ni.ac.rs*
[c]*Faculty of Mechanical Engineering, Niš, RS, milos.kocic@masfak.ni.ac.rs*
[d]*Faculty of Mecanical Engineering, Niš, RS, zivojin.stamenkovic@masfak.ni.ac.rs*

Abstract: EMHD flow and heat transfer of a ternary hybrid nanofluid is considered in this paper. The base fluid is blood with three types of nanoparticles suspended in it. Fluid flows in a horizontal channel with walls on different temperatures and its filled with porous medium. A homogeneous magnetic field acts perpendicular to the walls of the channel and a homogeneous electric field acts perpendicular to the direction of the magnetic field. The problem is considered in the induction-free approximation. The nanofluid velocity and temperature distributions, shear stresses and Nusselt numbers on the channel walls were determined. Some of the obtained results are presented graphically and tabularly.

Keywords: EMHD, Ternary hybrid nanofluid, Porous medium, Heat transport, Horizontal channel

1. Introduction

Convective heat transfer has significant applications in many industrial processes, as well as in biomedicine. That's why research is always present, the goal of which is to improve that process, and it is realized in different ways with more or less success. One way to realize these ideas is to improve the thermal conductivity of the working fluid. Since metals have a much higher thermal conductivity than fluids, the idea arose many years ago that the dispersion of metal particles in the fluid improves its thermal conductivity. However, only with the advancement of technology, Choi [1] was able to realize this idea, by dispersing nanometer-sized metal particles in a fluid and thus improving its conductivity and called this mixture a nanofluid. Since then, a large number of researchers have been dedicated to these fluids and their applications. Initially, one type of nanoparticles was dispersed in the fluid and these fluids are known as nanofluids (NF). It was later shown that better characteristics can be achieved by sputtering two types of nanoparticles and these fluids are known as chirid nanofluids (HNF). In recent years, fluids in which three types of nanoparticles are dispersed, which are known as three hydride nanofluids (THNF), have been investigated.

Many researchers indicate that heat transport of nanofluids in a porous medium in a magnetic environment is a relatively new area of research. A minimal number of fluid and nanofluid flow and heat transfer studies are cited here that sufficiently demonstrate how wide their distribution is. Lima et al. [2] investigated the magnetohydrodynamic (MHD) flow and heat transfer of two immiscible fluids in an inclined channel. They considered the effects of buoyancy, moving plates, layer porosity, tilted magnetic field, Joule and viscous dissipation, and heat generation/absorption. Raju and Satish [3] investigated the effect of slip on the electromagnetic hydrodynamic (EMHD) flow and heat transfer of two immiscible fluids in a horizontal channel including Hall currents. Nagavalli et al. [4] investigated the MHD flow of two immiscible, electrically conductive, incompressible fluids in a horizontal channel whose walls are horizontal plates. The canal walls are permeable. Hall currents are also taken into consideration. Unsteady MHD flow and heat transfer in a porous medium between two horizontal impermeable plates were investigated by Nikodijević et al. [5]. The applied magnetic field is inclined relative to the plates in the direction of the flow. Yadav et al. [6] investigated the effects of magnetic field and thermal radiation on entropy generation of immiscible micropolar and Newtonian fluids in a horizontal rectangular channel of a porous medium.

Manjeet and Sharma [7] investigated the MHD flow and heat transfer of an immiscible Newtonian and nanofluid (H_2O-Ag) in a horizontal channel with permeable walls. Umavathi and Oztop [8] performed a numerical simulation of EMHD flow and heat transfer of nanofluids in a vertical channel. The temperatures of the channel walls are constant, but different. EMHD flow and heat transfer of immiscible Newtonian and nanofluids in horizontal and vertical channels of porous media, respectively, were investigated by Petrović et al. [9, 10]. The channel walls were maintained at constant, but different temperatures. Devi et al. [11]

investigated the effect of different nanoparticles on unsteady MHD flow and heat transfer of two immiscible Newtonian and nanofluids in an inclined channel of porous medium and permeable walls. Petrović et al. [12] investigated the EMHD flow and heat transfer of Casson nanofluid Fe_3O_4-blood in a porous medium between two horizontal plates that are at constant but different temperatures. A study on NF including the most commonly used nanoparticles (NPs), improving thermal conductivity, improving stability, their impact on health and the environment, their application in biomedicine, etc. was presented by Hamad et al. [13].

Atay et al. [14] experimentally investigated the thermal characteristics of an aluminum microchannel cooler with rectangular sections, and NF TiO_2-water, Al_2O_3-ode and HNF Al_2O_3/ TiO_2-water were used as coolants. Algehne et al. [15] investigated the flow and heat transfer of THNF (TiO_2+MgO+$CoFe_2O_4$/EG) along a horizontal stretchable plate for industrial and biomedical applications. MHD flow of Williamson THNF with thermal radiation in a porous medium over a horizontal stretchable plate was investigated by Riaz et al. [16]. The effect of thermal radiation and magnetic dipole on the MHD flow of water-based NF, HNF and THNF on a stretching sheet was investigated by Nasir et al. [17]. MHD flow and heat transfer of a water-based THNF along a vertical stretching plate with thermal radiation, viscous dissipation, and ioconvection were investigated by Revathi et al. [18]. Raza et al. [19] investigated the effects of NP size and shape on the MHD flow and heat transfer of a THNF (Cu-Al_2O_3-TiO_2/H_2O) between two rotating permeable parallel plates.

By reviewing the available research, the authors of this paper are convinced that the simultaneous effects of magnetic field, electric field, shear, Joule and Darcy dissipation on the flow of THNF, whose base fluid is blood, have not been sufficiently investigated. Therefore, in this work, EMHD flow and mixed convection of THNF(Al_2O_3MgO+ TiO_2/blood) in a porous medium in a horizontal channel between two parallel stationary plates are investigated. The author's expectations are that this research will be applied later in biomedicine.

2. Mathematical formulation

In this paper, the flow of THNF in a porous medium whose permeability is K0 is considered, and it is located in a channel between two horizontal plates that are at an interzonal distance h. The plates are impermeable, and their temperatures are constant and amount to Tw1 on the top and Tw2 on the bottom. The applied external magnetic field is homogeneous perpendicular to the plate, and its induction is B. The applied external electric field is homogeneous, of strength E and is perpendicular to the longitudinal vertical plane of the channel. The physical configuration of the described problem with the selected coordinate system is shown in Figure 1.

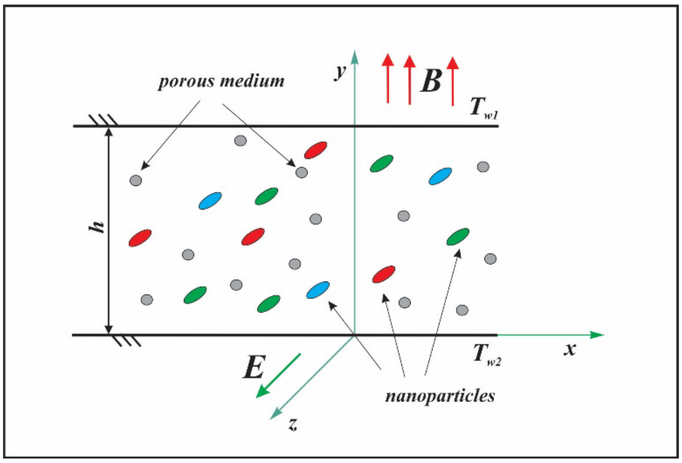

Figure 1

It is considered that the flow is stationary, laminar and fully developed, and the pressure gradient in the flow direction ∂p/∂X is constant. The problem is considered in the e-induction approximation, i.e. when the influence of the induced magnetic field can be neglected. The mathematical model of the described problem is described by the following equations and boundary conditions [7, 11]

$$-\frac{\partial p}{\partial X}+\mu\frac{\partial^2 U}{\partial Y^2}-\frac{\mu}{K_0}U-B\sigma\left(E+BU\right)=0, \qquad (1)$$

$$k\frac{d^2T}{dY^2}+\mu\left(\frac{\partial U}{\partial Y}\right)^2+\frac{\mu}{K_0}U^2+\sigma\left(E+BU\right)^2=0, \tag{2}$$

$$\left(U,T\right)\left(0\right)=\left(0,T_{w_2}\right),\left(U,T\right)\left(h\right)=\left(0,T_{w_1}\right), \tag{3}$$

in which the usual symbols were used, namely: X, Y – Descartes' coordinates, p, U, T – pressure, flow rate, temperature of THNF, respectively and μ, δ and k – physical properties of THNF, i.e. coefficient of dynamic viscosity, coefficient electrical conductivity and thermal conductivity coefficient, respectively.

It is assumed that the physical properties of THNF are invariable and the following known relations are used for them [15]:

$$\begin{aligned}
&\mu=\frac{\mu_f}{m},\ m=\left[\left(1-\Phi_1\right)\left(1-\Phi_2\right)\left(1-\Phi_3\right)\right]^{2.5};\\
&k=\varphi_2 k_f,\ \varphi_2=N\left(\Phi_3,k_3,k_f,\varphi_1\right),\ \varphi_1=N\left(\Phi_2,k_2,k_f,\varphi_0\right),\\
&\varphi_0=N\left(\Phi_1,k_1,k_f,1\right),\ N\left(\Phi,S,R,M\right)=\frac{\left(1+2\Phi\right)S+2\left(1-\Phi\right)RM}{\left(1-\Phi\right)S+\left(2+\Phi\right)RM};\\
&\sigma=\varphi_4\sigma_f,\ \varphi_4=N\left(\Phi_3,\sigma_3,\sigma_f,\varphi_3\right),\ \varphi_3=N\left(\Phi_2,\sigma_2,\sigma_f,\varphi_0^*\right),\ \varphi_0^*=N\left(\Phi_1,\sigma_1,\sigma_f,1\right).
\end{aligned} \tag{4}$$

In the last relations, indices 1, 2 and 3 in the properties and volume fraction ϕ of nanoparticles refer to the material properties and volume fractions of nanoparticles 1 and 3.

For further analysis of the problem described here, it is convenient to introduce the following dimensionless quantities:

$$y=\frac{Y}{h},\ u=\frac{U}{U_0},\theta=\frac{T-T_{w_2}}{T_{w_1}-T_{w_2}} \tag{5}$$

in which U_0 is the characteristic velocity given by the relation:

$$U_0=\frac{Ph^2}{\mu_f}, \tag{6}$$

where the label is introduced:

$$P=-\frac{\partial p}{\partial X}=const. \tag{7}$$

Using the introduced dimensionless quantities (5), equations (1), (2) and boundary conditions (3) are simply transformed to the following dimensionless equations and boundary conditions

$$\frac{d^2u}{dy^2}-\omega^2u=A, \tag{8}$$

$$\frac{d^2\theta}{dy^2}=-\frac{Br}{m\varphi_2}\left[\left(\frac{du}{dy}\right)^2+\omega^2u^2+Cu+D\right], \tag{9}$$

$$\left(u,\theta\right)\left(0\right)=\left(0,0\right),\ \left(u,\theta\right)1=\left(0,1\right). \tag{10}$$

In the last equations and boundary conditions, for the sake of brevity, the following symbols were used:

$$\begin{aligned}
&\Lambda=\frac{h^2}{K_0},Ha=Bh\sqrt{\frac{\sigma_f}{\mu_f}},K=\frac{E}{BU_0},\omega^2=\Lambda+m\varphi_4Ha^2,\\
&A=m\left(K\varphi_4Ha^2-1\right),C=2m\varphi_4Ha^2K,D=\frac{1}{2}CK,Br=\frac{\mu_f}{k_f}\frac{U_0}{T_{w_1}-T_{w_2}}
\end{aligned} \tag{11}$$

where: Λ-porosity factor, Ha-Hartmann's number, K-factor of electrical load, Br- Brinkman's number.

3. Solution

For further analysis of the problem described here, equations (8) and (9) with boundary conditions (10) should be solved. These equations can be solved analytically using a known mathematical method for solving linear differential equations. First, equation (8) is solved and then using that solution, which represents the distribution of the dimensionless flow velocity THNF, the solution of equation (9), i.e. the distribution of the dimensionless temperature of this fluid, is also determined.

The solution of equation (8) is given by the relation:

$$u(y)=C_1\exp(\omega y)+C_2\exp(-\omega y)+F, \tag{12}$$

in which C_1 and C_2 are integration constants and the introduced notation is:

$$F=-\frac{A}{\omega^2}. \tag{13}$$

Using the boundary conditions (10) for the dimensionless velocity, it is obtained that the integration constants are given by the relations:

$$C_1=E_1\left[\exp(-\omega)-1\right], C_2=\left[1-\exp(\omega)\right]. \tag{14}$$

where the label is used:

$$E_1=\frac{F}{\exp(\omega)-\exp(-\omega)}. \tag{15}$$

By substituting relation (12) in equation (9) and solving that equation, it is obtained that its solution is given by the relation

$$\begin{aligned}\theta(y)=-\frac{Br}{m\varphi_2}[&F_1\exp(2\omega y)+F_2\exp(-2\omega y)+R_1\exp(\omega y)+\\&R_2\exp(-\omega y)+R_3y^2+C_3y+C_4],\end{aligned} \tag{16}$$

in which C_3 and C_4 are integration constants, and the symbols used are:

$$\begin{aligned}&F_1=\frac{1}{2}C_1^{\,2}, F_2=\frac{1}{2}C_2^{\,2}, R_1=RC_1, R_2=RC_2,\\&R=\frac{1}{\omega^2}\left(C+2\omega^2F\right), R_3=\frac{1}{2}\left(D+CF+\omega^2F^2\right).\end{aligned} \tag{17}$$

Using the boundary conditions (10) for the dimensionless temperature, it is obtained that the integration constants are given by the relations:

$$\begin{aligned}&C_4=-F_1-F_2-R_1-R_2,\\&C_3=-\frac{m\varphi_2}{Br}-C_4-R_3-F_1\exp(2\omega)-F_2\exp(-2\omega)-R_1\exp(\omega)-R_2\exp(-\omega).\end{aligned} \tag{18}$$

Thus, relations (12) and (16) represent, respectively, the distributions of dimensionless velocity and dimensionless temperature THNF in the observed channel.

The dimensionless shear stresses on the left and right channel walls are given, respectively, by the relations:

$$\tau_1=\frac{\mu}{\mu_f}\left(\frac{du}{dy}\right)_{y=0}=\frac{\omega}{m}\left(C_1-C_2\right), \tag{19}$$

$$\tau_2=\frac{\mu}{\mu_f}\left(\frac{du}{dy}\right)_{y=1}=\frac{\omega}{m}\left[C_1\exp(\omega)-C_2\exp(-\omega)\right]. \tag{20}$$

The Nusselt numbers on the upper and lower channel walls, respectively, are represented by the relations:

$$N_{u_1} = \frac{k}{k_f}\left(\frac{d\theta}{dy}\right)_{y=0} = -\frac{Br}{m}\left[2\omega\left(F_1 - F_2\right) + \omega\left(R_1 - R_2\right) + C_3\right] \tag{21}$$

$$N_{u_2} = \frac{k}{k_f}\left(\frac{d\theta}{dy}\right)_{y=1} = -\frac{Br}{m}\left\{2\omega\left[F_1 \exp(2\omega) - F_2 \exp(-2\omega)\right] + \omega\left[R_1 \exp(\omega) - R_2 \exp(-\omega)\right] + 2R_3 + C_3\right\} \tag{22}$$

4. Analysis of results

The results of dimensionless velocity and dimensionless temperature THNF, as well as dimensionless shear stresses and Nusselt numbers on channel walls, determined in the previous chapter, depend on the introduced physical factors that are significant for flow and heat transfer in the problem considered here. Therefore, they have generality because they refer to any THNF, not just one specific one, as well as to channels of different porosities that are in the environment of different magnetic and electric fields. They can be used for any THNF as well as for cases of different porosity of the channel medium and different magnetic and electric fields.

In this chapter, the flow and heat transfer of THNF whose base fluid is blood and nanoparticles are aluminum oxide (Al_2O_3), magnesium oxide (MgO) and titanium dioxide (TiO_2) are considered. The physical properties of the blood and nanoparticle materials used here are given in Table 1.

Part of the results obtained here for the distributions of dimensionless velocity and dimensionless temperature are given in the following figures, for several values of the introduced physical factors, in the form of graphs. Part of the results for dimensionless vertical shears on channel walls and Nusselt numbers on them are given in Table 1.

Table 1. Physical properties

Supstance properties	blood	Al_2O_3	TiO_2	MgO
$\rho\left(kg/m^3\right)$	997.1	3970	4250	3560
$c_p\left(J/(kgK)\right)$	4179	765,	686.2	955
$K\left(W/(Km)\right)$	0.613	40	8.9538	45
$\sigma\left(S/m\right)$	5.5×10^{-6}	35×10^{6}	2.6×10^{6}	5.392×10^{-7}
$\mu\left(Pas\right)$	0.001	-	-	-

Here the results are given for the values of the parameters Br=0.3, Ha=, K= -1, Λ=, $\phi_1 = \phi_2 = \phi_3 = 0.01$ and the value of the parameter whose influence is analyzed is changed.

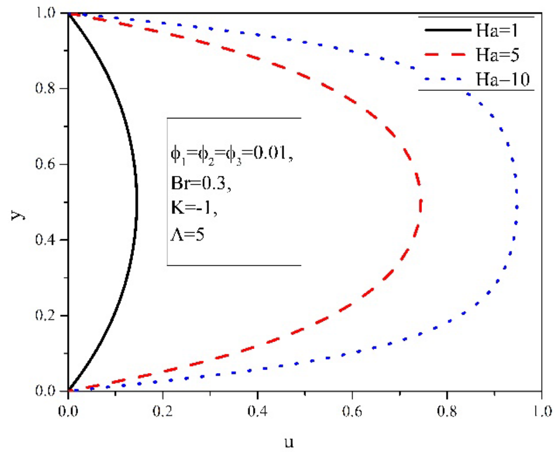

Fig. 2 Velocity distributions for different Ha values

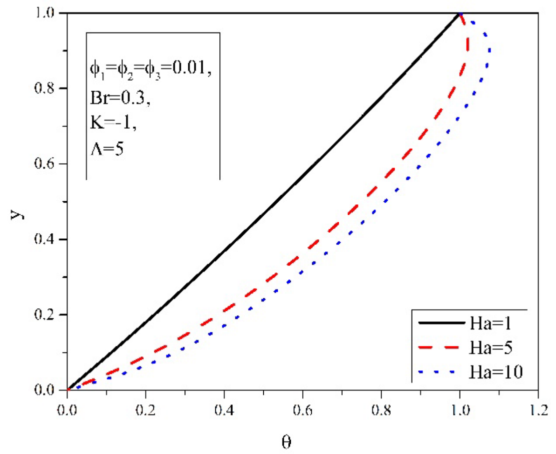

Fig. 3 Temperature distributions for different Ha values

Fig. 2 and Fig. 3 show distributions of speed and temperature of THNF in the channel for different values of the Ha number, respectively. Fig. 2 shows that an increase in the value of Hartmann's number increases the speed of fluid flow in the channel. The reason for this increase in speed is the increase in the intensity of the Lorentz force, which, in this case, is the driving force. The velocity distributions are symmetrical with respect to the horizontal plane of the middle of the channel. Fig. 3 shows that an increase in the value of the Ha number leads to an increase in the temperature of the fluid in the channel. This particle is physically explained by the increase in Joule's heat. For values of Ha=1, heat transfer is mainly by conduction. For the values of Ha= and Ha=10, the heat transfer is from the fluid to the upper channel wall.

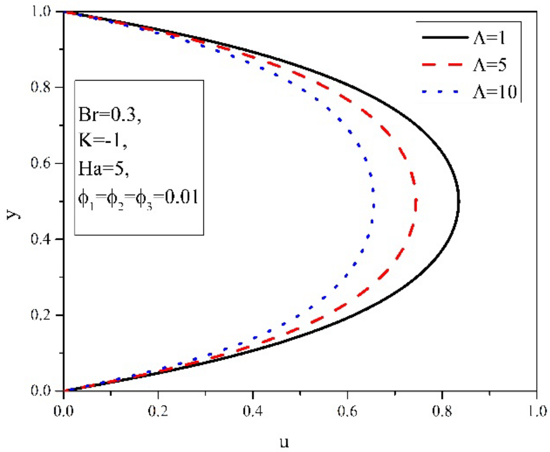

Fig. 4 Velocity distributions for different Λ values

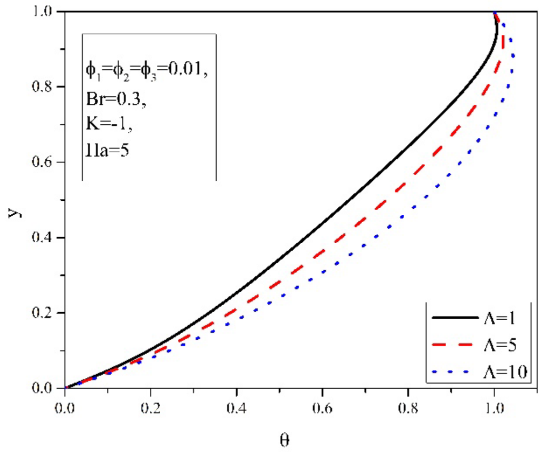

Fig. 5 Temperature distributions for different Λ values

In fig. 4 and 5 graphs of the distribution of fluid velocity and temperature in the channel for different values of the porosity factor (Λ), respectively, are given. It can be seen from Fig. 4 that higher values of Λ correspond to lower fluid flow speeds in the channel. The reason for this decrease in speed is the increase in the intensity of the Darcy force, which is the force of resistance to fluid flow. And in this case, the graphs of the speed distribution are symmetrical. Fig.5 shows that an increase in the value of Λ leads to an increase of temperature in the channel. This conclusion is physically explained by the increase in Darcy dissipation. For all three values of Λ, heat transport is from the fluid to the upper channel wall.

Distributions of fluid speed and temperature in the channel for different values of the external electrical load (K) are graphically presented in Fig. 6 and Fig. 7, respectively.

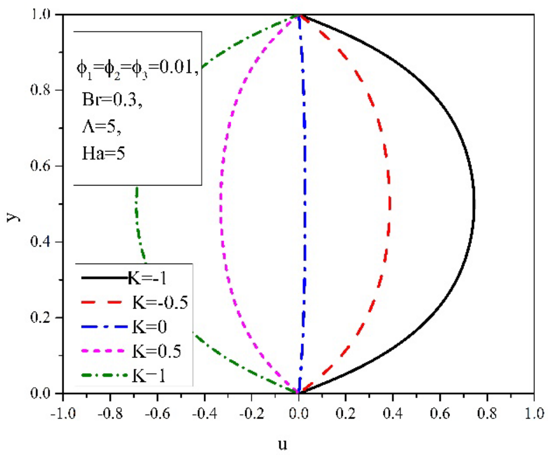

Fig. 6 Velocity distributions for different K values

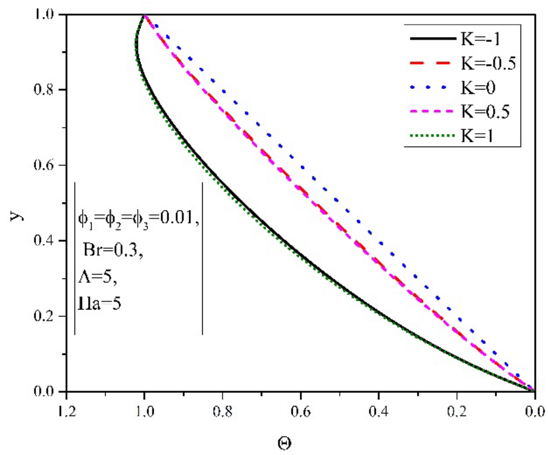

Fig. 7 Temperature distributions for different K values

Fig. 6 shows that larger values of |K| higher velocities correspond, while changing the sign of the factor K changes the direction of fluid flow. This conclusion is physically explained by the fact that for K<0 it is the Lorentz driving force, and for K>0 it is the force of resistance to fluid flow and that its intensity is higher for higher values of |K|. Fig. 7 shows that larger values of |K| correspond to higher fluid temperatures in the channel. This is physically explained by Joule heat transfer. For K=0 heat transfer is mainly by conduction.

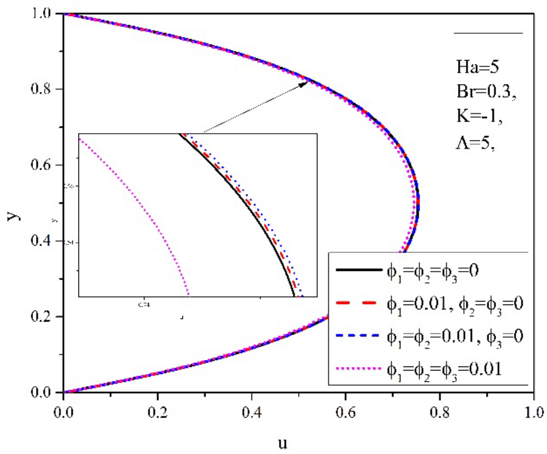

Fig. 8 Velocity distributions for different ϕ values

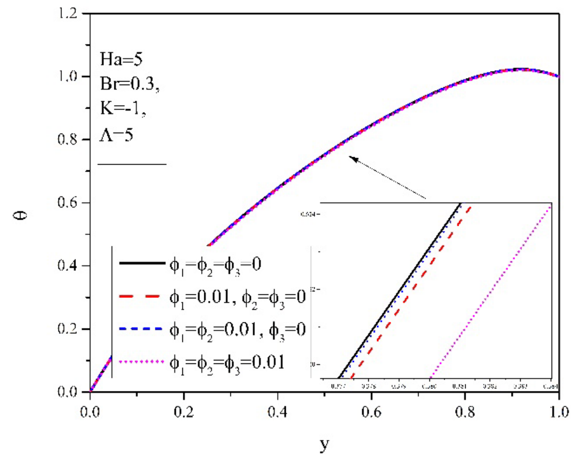

Fig. 9 Temperature distributions for different ϕ values

For base fluid (blood) ($\phi_1= \phi_2= \phi_3=0$), NF ($\phi_1=0.01$, $\phi_2= \phi_3=0$), HNF($\phi_1= \phi_2= 0.01$, $\phi_3=0$) and THNF ($\phi_1= \phi_2= \phi_3= 0.01$) graphs of distribution of velocity and temperature of the fluid in the channel are presented in fig. 8 and Fig. 9, respectively. It can be seen, from Fig.9, that the speed is the lowest when THNF is flowing in the channel. This can be physically explained by the fact that the fluid is denser, has a higher coefficient of dynamic viscosity, and then the force of resistance to the flow due to viscosity is more intense. From fig.10, it can be seen that the temperature is the lowest when the THNF flows, which can be explained by the improved thermal conductivity.

Table 2 gives the values of shear stress and Nusselt numbers on channel walls for different values of the introduced influential physical parameters. From this table, it can be seen that higher values of the Ha number correspond to higher values of shear stress on the channel walls and higher values of Nusselt swarm on the bottom wall of the channel. On the upper wall of the channel for Ha=1 is $Nu_2>0$, which means that heat transport is from the wall to the fluid. For the values of Ha=5 and Ha=10, $Nu_2<0$ and is greater than the absolute value for a greater value of Ha, which means that heat transport is greater for a greater value of Ha swarm.

Higher values of |K| correspond to higher values of the shear stress on the channel walls and higher values of the Nu_1 number. On the upper wall of the channel, the value of the Nu_2 number is the highest for K=0.

Table 2. Values of shear stresses and Nusselt numbers

	τ_1	τ_2	Nu_1	Nu_2
Ha=1	0.03415	-0.032	1.24266	0.930317
Ha=5	4.974293	-4.97429	2.951512	-0.77853
Ha=10	10.45318	-10.4532	4.810593	-2.6361
K=-1	4.974293	-4.97429	2.951512	-0.7853
K=-0.5	2.578781	-2.57878	1.555005	0.617974
K=0	0.183269	-0.18327	1.089503	1.083476
K=0.5	-2.21224	2.212243	1.555005	0.617974
K=1	-4.60775	4.607754	2.951512	-0.77853
Λ =1	5.331527	-5.33153	2.724674	-0.5517
Λ=5	4.974293	-4.97429	2.951512	-0.77853
Λ=10	4.611617	-4.61162	3.177669	-1.00469
$\phi_1= \phi_2= \phi_3= 0$	4.974293	-4.97429	2.951512	-0.77853
$\phi_1=0.01$ $\phi_2= \phi_3= 0$	4.835459	-4.83546	2.838311	-0.77991
$\phi_1= \phi_3=0$ $\phi_2= 0.01$	4.835459	-4.83546	2.834873	-0.78335
$\phi_1= \phi_2=\phi_3= 0.01$	4.974293	-4.97429	2.951512	-0.77853

Higher values of the factor Λ correspond to smaller values of the shear stress on the channel walls, higher values of the Nu_1 number and higher absolute values of the Nu_2 number. For the values of Λ given here, on the upper wall of the channel is heat transport from the fluid to the wall.

5. Conclusion

In this paper, the electromagnetic hydrodynamic flow and heat transfer of a ternary hyridic nanofluid in a horizontal channel saturated with a porous medium is considered. Analytical distributions of velocity and temperature in the channel and shear stresses and Nusselt numbers on the channel walls were determined. Part of the obtained results for the case of the ternary hybrid nanofluid (Al_2O3+MgO+TiO_2 /blood) is given in the form of graphs and tables. Based on the analysis of the obtained results, appropriate conclusions were drawn. It was concluded that an increase in the value of Hartmann's number leads to an acceleration of the fluid flow in the channel and to an increase in its temperature. Increasing the value of the factor Λ ie. the decrease in the permeability of the porous medium slows down the fluid flow in the channel and causes an increase in its temperature. Larger absolute values of the external electrical load factor lead to an acceleration of the flow and an increase in the temperature of the fluid in the channel. Changing the sign of the factor K leads to a change in the direction of fluid flow. Flow is slowest when in the THNF channel compared to flow when in the HNF, NF or base fluid channel.

Acknowledgements

This research was financially supported by the Ministry of Education, Science and Technological Development of the Republic of Serbia.

References

[1] CHOI S.U.S. (1995) Enhancing thermal conductivity of fluids with nanoparticles, Developments and Applications of Non-Newtonian Flows, MD vol. 231 and FED vol. 66 ASME, pp. 95-105.

[2] LIMA J. A., ASSAD G. E. and PAVIA H. S. (2016) *A simple approach to analyze the fully developed two-phase magnetoconvection type flows in inclined parallel-plate channels*, Latin American Applied Research, 46(3), pp. 93-98, doi:10.52292/jaar.2016.333

[3] T.Linga Raju and P. Satish (2023), Slip regime MHD 2-liquid plasma heat transfer flow with Hall currents between parallel plates, Int. J. Of Applied Mechanics and Engineering, vol. 28, No. 3, pp. 65-85, doi:10.59441/ijame/172898

[4] Nagavali, M., Linga Raju, T., Kameswaran, P. K.(2022). Two-Layered Flow of Ionized Gases ithin a Channel of Parallel Permeable Plates Under an Applied Magnetic Field with the Hall Efect. In: Rushi Kumar, B., Pannusamy, S., Giri, D., Thuraisingham, B., Clifton, C.W., Carminati, B.(eds) Mathematics Computing. ICMC2022. Springer Proceedings in Mathematics and Statistics, vol. 41, Singapore, doi: 10.1007/978_981_19_9307_7_43.

[5] Milica Nikodijević, Živojin Stamenković, Jelena Petrović, Miloš Kocić, (2020), Unsteady Fluid Flow and Heat Transfer Through a Porous Medium in a Inclined Magnetic Field, Transactions of Famena, Vol. 44(4), pp. 31-46, doi:10.21278/TOF.444014420

[6] Aaiza Gul, Ilyas Khan and Sharidan Shafie (2018), Radiation and Heat generation effects in magnetohydrodynamic mixed convection flow of nanofluids, Thermal Science, Vol. 22, No. 1A, pp. 51-62, doi:10.2298/TSCI150730049G

[7] Manjet and Mukesh Kumar Sharma (2020), MHD flo and heat Convection in a channel filled with two immiscile newtonian and nanofluid fluids, JP Journal of Heat and Mass Transfer, Volume 21, Numer 1, Pages 1-21, doi: 0.17654/HM021010001

[8] J.C.Umavathi and Hakan F.Oztop (2021), Investigation of MHD and applied electric field effects in a conduit cramed with nanofluids, International Communications in Heat and Mass Transfer, Vol. 121:105097, doi:10.1016/j.icheatmasstransfer.2020.105097

[9] PETROVIĆ J.D., STAMENKOVIĆ Ž., BOGDANOVIĆ JOVANOVIĆ J:, NIKODIJEVIĆ M., KOCIĆ M., NIKODIJEVIĆ D. (2022) *Electro-Magneto Convection Immiscible Pure Fluid and Nanofluid*, Transactions of FAMENA 46(3):13-28, doi:10.21278/TOF.463036021

[10] Jelena D. Petrović, Živojin Stamenković, Miloš Kocić, Milica Nikodijević, Jasmina Bogdanović Jovanović, Dragiša D. Nikodijević (2022), Magnetohydrodynamicflow and mixed convection of a viscous fluid and a nanofluid a porous medium in a vertical channel, Thermal Science Volume 27, Issue 2 Part B, pp. 1453-1463, doi:10.2298/TSCI220903188P

[11] M.Padma Devi, Kamal Goyal, S. Srinivas, B. Satyanarayana (2024), Effects of different nanoparticles on the two immiscible liquids flow in an inclined channel with Joule heating and viscous dissipation, Gulf Journal of Mathematics Vol. 16, Issue 2, 278-290, doi:10.56947/gjam.V16i2.1815

[12] Petrović D. Jelena, Nikodijević Đorđević Milica, Kocić Miloš, (2023), Electromagnetic hydrodynamic flow and heat transfer of a Casson nanofluid Fe_3O_4-blood in a porous medium, Thermal Science Volume 27, Issue 6 Part A, pp. 4461-4472, doi:10.2298/TSCI230516169P

[13] Eyad M. Hamad, Aseel Khaffaf, Omar Yasin, Ziad Au El-Rub, Samer Al-Gharabli, ael Al-Kouz and Ali J. Chamkha (2021, Revie of Nanofluids and Their iomedical Applications, Journal of Nanofluids, Vol. 10, pp. 63-, doi: 10.1166jon.2021.1806
[14] Mohammad Ataei, Farhad Sadegh Moghanlou, Saeed Noorzadeh, Mohammad Vajdi and Mehdi Shahedi, (2020), Heat transfer and flo characteristics of hrid Al_2O_3/T_iO_2-water nanofluid in a minichannel heat sink, Heat and Mass Transfer Volume 6, issue 9, pp. 2757-2767, doi: 10.100/s00231-020-02896-9
[15] Ebrahem A. Algehyne, Haiffa F. Alrihieli, Muhammad Bilal, Anwar Saeed and Wajaree Weera (2022), Numerical Approach toward Ternary Hybrid Nanofluid Flow Using Variable Diffusion and Non-Fouriers Concept, ACS Omega 7 (33), 29380-29390, doi:10.1021/acsomega.2c03634
[16] Saman Riaz, Muhammad F.Afzaal, Zhan Wang, Ahmed Jan and Umer Farooq (2023), Numerical heat transfer of non-similar ternary hybrid nanofluid flow over lineary stretching surface, Numerical Heat Transfer, Part A: Applications, doi:10.1080/10407782.2023.2251093
[17] Saleem Nasir, Sehson Sirisubtawee, Pongpol Juntharre, Adallah S Berrouk, Safyan Mukhtar, Taza Gul (2022), Heat transport study of ternary hyrid nanofluid flow under magnetic dipole together with nonlinear thermal radiation, Applied Nanoscience 12(2), doi:10.1007/s13204-022-02583-7
[18] Gadamsetty Revathi, Isac Lare Animasaum, Venkata Surbahmanyam Sajja, Macherla Jayachandra Babu, Naresh Boora and Shakravarthula S. K. Raju (2022), Significance of adding titanium dioxide nanoparticles to an existing distilled water conveying aluminium oxide and zinc oxide nanoparticles: Scrutinizstion of chemical reactive ternary hyrid nanofluid due to bicconvection on a convectively heated surfface, Nonlinear Engineering 11; 21-251, doi: 10.1515/nleng-2022-0031
[19] Qadeer Raza, Xiaodong Wang, Hussein A. H. Muhammed, Bagh Ali, Mohamed R. Ali, Ahmed S. Hendy (2024), Numerically analyzed of ternary hybrid nanofluids fflow of heat and mass transfer subject to various shapes and size factors in two-dimensional rotatting porous channel, Case Studies in Thermal Engineering 56, 104235, doi: 10.1016/j.csite.2024.104235